Available online at www.sciencedirect.com

ScienceDirect

Journal of Photochemistry and Photobiology A: Chemistry 195 (2008) 307–313

Journal of Photochemistry and Photobiology A:Chemistry

www.elsevier.com/locate/jphotochem

Commercial and natural dyes as photosensitizers for a water-based dye-sensitized solar cell loaded with gold nanoparticles

Wei Hao Lai [a,1], Yen Hsun Su [b,2], Lay Gaik Teoh [c,*], Min Hsiung Hon [a,3]

[a] *Department of Materials Science and Engineering, National Cheng Kung University, Tainan 70101, Taiwan*
[b] *Department of Physics, National Cheng Kung University,Tainan 70101, Taiwan*
[c] *Department of Mechanical Engineering, National Pingtung University of Science and Technology, Neipu, Pingtung 91201, Taiwan*

Received 13 February 2007; received in revised form 23 October 2007; accepted 30 October 2007

Abstract

We fabricated gold nanoparticles as a Schottky barrier on a TiO_2 electrode, which adsorbed the commercial dyes and free natural dyes in the water-based dye-sensitized solar cell (water-based DSSC) with the aqueous electrolyte of $Ce^{4+/3+}$ system. Conversion of visible light into electricity was accomplished with natural dyes, resulting in excellent photoelectric properties compared to those achieved with commercial dyes. The extracts of the natural dye *Rhoeo spathacea* (Sw.) Stearn. can reach the solar conversion efficiency of 1.49%, which had the best photosensitized effect of the water-based DSSC. Due to the simple preparation technique, wide availability and low cost, natural dyes are promising as environmentally friendly alternative sensitizers for water-based DSSC.

Keywords: Dye-sensitized solar cell (DSSC); Gold nanoparticle (Au NP); Chlorophyll; Schottky barrier; Photoluminescence

1. Introduction

Dye-sensitized solar cells (DSSCs) are devices for the conversion of visible light into electricity based on sensitization of wide bandgap semiconductors. The sensitization approach enables the generation of electricity with irradiation of energy lower than the bandgap of the semiconductor [1]. The progress of such devices occurred with the development of nanostructured semiconductor films onto which light absorbing dye molecules are adsorbed [2,3]. Many efforts have focused on sensitizer dye, since dye plays a key role in harvesting sunlight and transforming solar energy into electric energy [4]. Several organic dyes and organic metal complexes have been employed to sensitize nanocrystalline TiO_2 semiconductors, and one of the most efficient sensitizers is a transition metal coordination compound (e.g. ruthenium polyridyl complex). This is because the complex has intense charge-transfer absorption in the whole visible range, a long excitation lifetime and highly efficient metal-to-ligand charge transfer.

Among several kinds of DSSCs, the water-based DSSC is a good candidate for use in nontoxic and biologically friendly solar energy devices. The development of an environmentally friendly method for preparation of advanced DSSC is thus desirable. Except for the early experiments of Grätzel et al. [5], little study has been attempted on the construction of water-based DSSCs, because aqueous electrolytes generally yield very low conversion efficiency (<1%) compared with organic electrolytes. However, Murakami et al. [6] yielded high conversion efficiency for water-based DSSC with water or ethanol as an electrolyte when using N719 as a dye.

Gold nanoparticles (Au NPs) have unusual chemical [7,8] and physical properties [9,10], such as catalytic activity, novel electronic, optical, magnetic, and biosensing properties, as well as potential applications in solar cells [11–13]. When light absorption takes place, electron injection from the excited dye to the conduction band of the semiconductor may occur on an ultrafast time scale. Au NPs can act as a Schottky barrier [14–16] which promotes the efficiency of the photoelectric conversion in water-based DSSC. A Schottky barrier can be formed in the interfacial region of the Au and the semiconductor in the solar

---

[*] Corresponding author. Tel.: +886 87703202x7525; fax: +886 87740142.
E-mail address: n5888107@mail.npust.edu.tw (L.G. Teoh).
[1] Tel.: +886 912720296.
[2] Tel.: +886 912012204.
[3] Tel.: +886 62757575x62932; fax: +886 62380208.

1010-6030/$ – see front matter © 2007 Elsevier B.V. All rights reserved.
doi:10.1016/j.jphotochem.2007.10.018

cell device, and the efficiency of the electron injection will then be increased [15,16]. The Au NP's layer is thus used to create a Schottky barrier between the Au and the semiconductor oxide. The transportation of concentration-driven electrons is slow between the dye and electrode without the Schottky barrier. When an electron in the lowest unoccupied molecular orbital of the dye passes the Au thin layer through tunneling to the conduction band of the TiO_2, it is unable to go back to either the dye or the electrolyte due to the Schottky barrier. However, a water-based DSSC has no Schottky barrier to yield the efficiency, and N719 is very expensive. The fabrication of Au NPs on the electrode is one cost-effective way to produce the Schottky barrier in water-based DSSC, but most work on this does not report on the resulting efficiency, although Prof. Tatsuma et al. have published several excellent papers about Au NP-sensitized TiO_2 solar cells [16–19] which reveal the feasibility and applications of Au NPs in water-based DSSC.

For the first time we have fabricated a Au NP's layer loaded on the TiO_2 of photoelectrode of water-based DSSC. The efficiency of photoelectric conversion is measured with/without Au NPs, and it achieves the effect of a Schottky barrier [20]. In the aqueous electrolyte of the $Fe^{2+/3+}$ system, the short-circuit current of water-based DSSC without Au NPs (2.76 mA/cm^2) is lower than that with the layer of Au NPs (5.96 mA/cm^2). Au NPs acting as a Schottky barrier can enhance the electric current of DSSC. The filling factor of water-based DSSC with Au NPs (34.9%) is higher than that without them (23.0%). The efficiency of solar cells can also be increased when the anode electrode is coated with Au NPs. The efficiency of photoelectric conversion of water-based DSSC with Au NPs (0.95%) is higher than that without them (0.26%). The layer-by-layer Au NPs film is thus suitable to be applied in the field of water-based DSSC [20]. In this report, the commercial dyes of crystal violet, mercurochrome, and chlorophyll act as inexpensive and biologically friendly photosensitizers. The present work further extends our investigations involving natural dyes as cost-free photosensitizers and reports the successful use of extracts of *Bongainvillea brasiliensis* Raeusch., *Garcinia suubelliptica.*, *Ficus Reusa* Linn., and *Rhoeo spathacea* (Sw.) Stearn. loaded on the Au NPs in water-based DSSC. These four natural dyes are all widely disseminated over Taiwan. The aqueous electrolyte of the $Ce^{4+/3+}$ system, which has lower potential than the I_3^-/I^- system [21] to improve the photoelectric conversion efficiency, was also first reported in the water-based DSSC. Due to their simple preparation techniques, wide availability and low cost, natural dyes are promising alternative sensitizers for water-based DSSC, potentially applicable for use in environmentally friendly solar energy devices.

2. Experimental

2.1. Preparation of the photoelectrodes of water-based DSSC

12 g of P-25 TiO_2 (Degussa, Japan) powders in 15 ml of DI-water mixed with 0.2 ml of Triton-X 100 (Sigma Chemical Co., USA) and 0.4 ml of Acetylaceton (99.5%, Fluka, Germany) was vibrated ultrasonically for 3 days. 0.5 ml of TiO_2 solution was then spin coated on fluorine-doped tin oxide (FTO glass, 8 Ω/cm^2, made by Solaronix Sa, Swiss) substrate (2 cm × 2 cm) as the anodic photoelectrode of water-based DSSC with 1000 rad/s for 20 s. TiO_2 paste with an area of about 0.5 cm × 0.5 cm and thickness of 1.8 μm was spread onto the conductive FTO glass substrate. After calcinations at 500 °C for 10 h, P-25 had higher anatase content (rutile/anatase = 1:4) [22]. The cathodic photoelectrode of water-based DSSC was prepared by sputtering silver on the indium-doped tin oxide (ITO) glass substrate.

2.2. Preparation of gold nanoparticles

Au NPs were synthesized by chemical reduction method. 3 mM of $HAuCl_{4(aq)}$ (Alfa Aesar Chemical Co., UK) 30 ml was added into 5 mM of tetraoctylammonium bromide (TOAB) (Sigma Chemical Co., USA) and 80 ml in hexane. In addition, 0.05 M of $NaBH_{4(aq)}$ (Alfa Aesar Chemical Co., UK) 25 ml was added to the former solution, and the color turned from yellow to black. Au NPs were modified by tetraoctylammonium bromide. The anodic photoelectrode of water-based DSSC was immersed in Au NPs colloid solution for 48 h.

2.3. Preparation of dye sensitizers and adsorption of dyes on the photoelectrode of water-based DSSC

A variety of commercial and natural dye sensitizers were adopted in this study. The commercial dyes selected in this investigation were methyl violet (99%, Showa Chemical Co., Japan), mercurochrome (99%, Showa Chemical Co., Japan), and chlorophyll (Tokyo Chemical Industry Co., Japan) mixed in alcohol solution (17.5 μM). The natural dye sensitizers were also prepared in alcohol. The alcohol extracts of *Bongainvillea brasiliensis* Raeusch., *Garcinia suubelliptica.*, *Ficus Reusa* Linn., *Rhoeo spathacea* (Sw.) Stearn. were obtained according to the following steps: the clean fresh samples of *Bongainvillea brasiliensis* Raeusch., *Garcinia suubelliptica.*, *Ficus Reusa* Linn., *Rhoeo spathacea* (Sw.) Stearn. and kelp were dried at 40 °C in a vacuum drying oven; after crushed into a fractionlet, the raw materials of 0.5 g/100 ml were put into a 95 wt% ethanol solution and kept in ambient temperature without exposure to direct sunlight for several weeks to adequately extract natural dye in the solution, solid residues were filtrated out and the natural dye solutions were concentrated to one-quarter with a rotatory evaporator at 40 °C, then the natural dye solutions were refined by the chromatogram method. After that, the natural dye sensitizer alcoholic solutions (17.5 μM) were prepared.

2.4. Assembly of water-based DSSC

The anodic photoelectrode of water-based DSSC loaded with Au NP's layer was immersed in various dye sensitizer alcohol solutions for 2 days. The electrolyte was the water-based solution (35% ethanol and 65% water), including 0.1 M $Ce(NO_3)_3$/0.05 M $Ce(NO_3)_4$ (99%, ICN Biomedicals, Inc.,

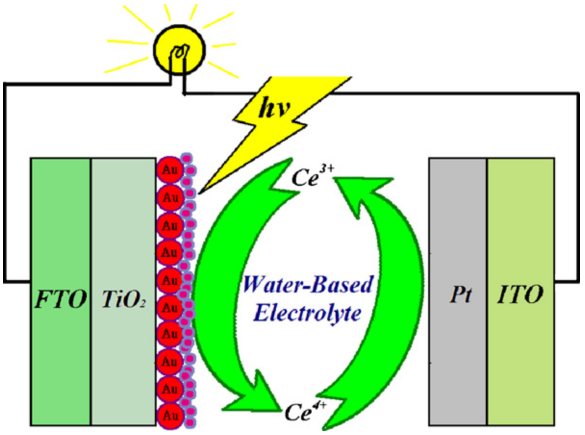

Fig. 1. Electric circuit system of water-based dye-sensitized solar cell (● : dye).

USA). The assembly of the rectangular-shaped water-based DSSC is schematically depicted in Fig. 1.

2.5. Instruments and measurements

The morphologies of Au NPs were observed by TEM. The as-grown product was observed with a Hitachi model HF-2000 transmission electron microscope operating at 200 kV. The transmission spectrum of the photoelectrode with Au NP's layer and the absorption spectra of dyes were determined by UV–vis spectrum (Hitachi U-2001 spectrophotometer, Japan). The samples were directly injected into a quartz tube for UV–vis analysis. The photoluminescence (PL) spectra of the samples were analyzed with a Fluorescence Spectrophotometer (Hitachi F-4500 FL Spectrophotometer, Japan). The photocurrent conversion efficiency was measured in the dark without a photo-mask and under simulated solar irradiation of one sun intensity (AM 1.5G) with the irradiated area of the entire photoelectrode (about 4 cm^2). The fill factor was calculated at 100 mW/cm^2 by dividing the maximum product of current and voltage from the illumination.

3. Results and discussion

3.1. Gold nanoparticles as a Schottky barrier in water-based DSSC

The shape of Au NPs modified by TOAB in hexane is close to sphere-like, as shown in Fig. 2. The average size of the Au NPs is about 6 nm. The nano-beam diffraction pattern of Au NPs is the standard indexed diffraction pattern for face center cubic (FCC) crystals in the [0 1 1] beam direction, as seen in the inset of Fig. 2. From TEM observation, Au NPs are poly-crystals, and the grain boundary can be seen.

The transmission of with and without Au NP's layer adsorbed on the TiO_2 photoelectrode is shown in Fig. 3. The thickness of the Au NP's layer is about 38 nm. The transmission of the photoelectrode with an Au NP's layer is slightly lower than that without. The difference of photoelectrode transmission with and without the Au NP's layer is 9% at the infrared region, and 11% at the surface plasmons of Au NPs (520 nm). The maximum transmission of the Au NP's layer adsorbed on the TiO_2 photoelectrode is about 90%, which reveals excellent transmission of the TiO_2 photoelectrode with adsorption of Au NPs and thus use in suitability for the assembly of a water-based DSSC device.

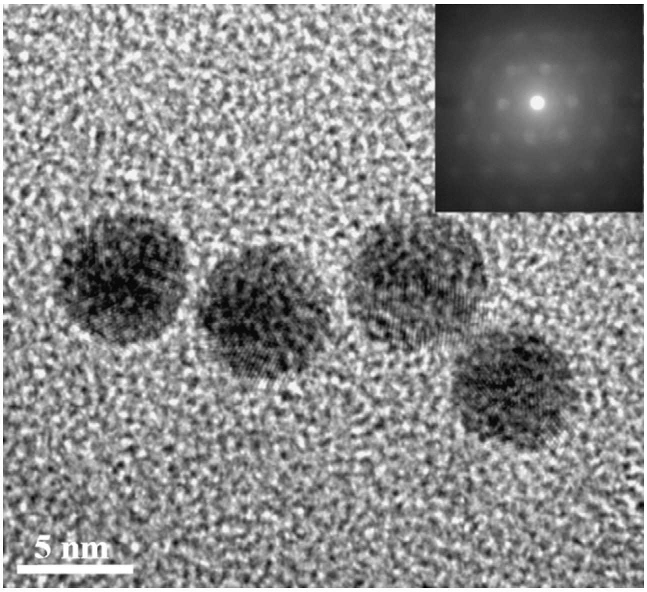

Fig. 2. TEM image and diffractive pattern (inset) of Au nanoparticles in hexane.

The existence of the Schottky barrier can be found by McFarland and Tang [14], which fabricates a multilayer structure that physically separates the processes of light absorption and charge-carrier transport. If electrons moving from semiconductor to the metal are retarded by the Schottky barrier, the resulting equation in the dark field will be given as follows [23]:

$$\ln I = \ln I_0 + \frac{qV}{kT} \tag{1}$$

where I is the current, I_0 is the initial current, q is the charge carrier, V is the input voltage, k is the Boltzmann's constant, and T is the absolute temperature. In this study, the correlation between applied voltage (V) and the Napierian logarithm of current (ln J) with Au NP's layer adsorption on the TiO_2 photoelectrode is

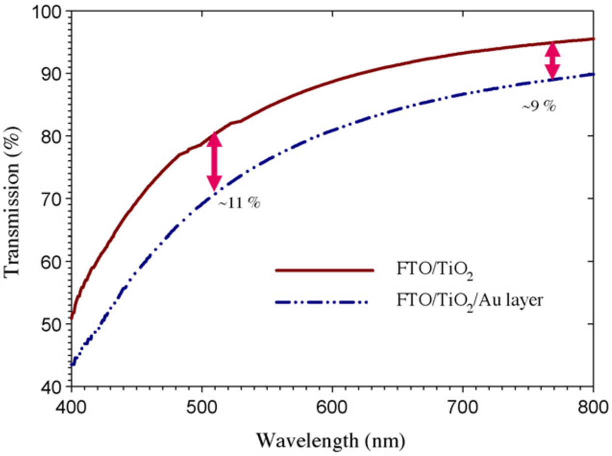

Fig. 3. Transmission of with and without Au NP's layer adsorbed on the TiO_2 photoelectrode.

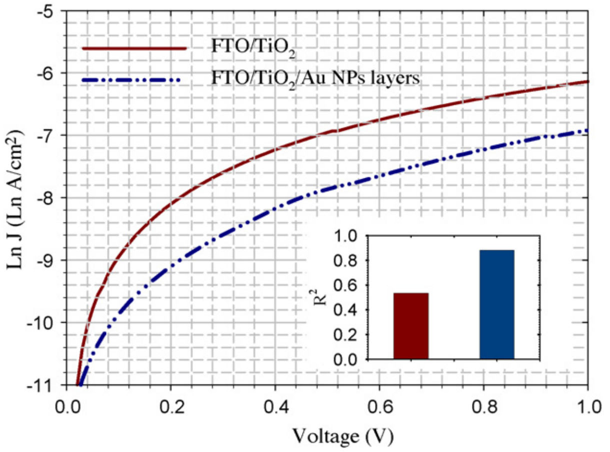

Fig. 4. ln *J*–*V* curve and relative coefficient (inset) for absorption of Au NPs loaded on TiO_2 layer in the dark field for the water-based DSSC.

a linear relationship (blue curve in Fig. 4) in the dark field. The linear relation ranges from 1 to 0.3 V. The relative coefficient (in the inset of Fig. 4) of the linear regression for the Au NP's layer (0.88) is better than that without the Au NP's layer (0.54). From the *J*–*V* curve in Fig. 4, we can conclude that the change of electric property with and without the Au NP's layer can be correlated with the Schottky barrier between the interfacial regions of the dye and the semiconductor film (i.e. TiO_2 photoelectrode) in the solar cell device. After light absorption by dye molecules charge separation can occur, followed by the electron transfer process. In this process, the electronically excited dye molecule acts as a primary electron donor and the semiconducting electrode is an electron acceptor [24]. The layer of Au NP's plays the role of a secondary electron donor, and provides an electron in order to make the dye molecule return to its ground state. Therefore, the Au NP's layer was adsorbed on the TiO_2 photoelectrode as the Schottky barrier in water-based DSSC. We applied Ellipsometry to explore the evidence that the Au NP was dispersed on the TiO_2 photoelectrode. The maximum fraction of layer-by-layer Au NPs is about 60% when the number of Au NP layers is more than three. The mean-square-error (MSE) values are less than 1 [20]. In this report, the maximum fraction of Au NPs by the immersed method is about 85% and MSE values are less than 0.1. The Au NPs were homogeneously dispersed in the TiO_2 layer.

3.2. Absorption spectra of various kinds of the commercial and natural dyes in the water-based DSSC

In the spectroscopic research stage, the absorption spectra of dyes are always monitored and they provide information on the probability of the absorption transition between the dye ground and excited states and the energy range of solar energy absorbed by the dye species [24]. Fig. 5a shows the UV–vis absorption spectra of three kinds of commercial dyes (crystal violet, mercurochrome, and chlorophyll) and Fig. 5b four kinds of natural dyes (*Bongainvillea brasiliensis* Raeusch., *Garcinia suubelliptica.*, *Ficus Reusa* Linn., and *Rhoeo spathacea* (Sw.) Stearn.), with kelp extracts in alcohol. Considering the absorption spectra of the three kinds of commercial dyes in Fig. 5a, mercurochrome has the largest absorption peak, with the wavelength of 515 nm, and crystal violet shows its maximum absorption at λ_{max}: 588 nm [25]. Meanwhile, chlorophyll absorbs most strongly in the blue and red portions of the absorption spectrum, but poorly in the green, hence the green color of chlorophyll-containing tissues, such as plant leaves. The absorption peaks of chlorophyll α are at 665 and 430 nm. The shift of the absorption bands can usually be due to the delocalization of π electrons in the conjugated molecular system and/or to aggregation of dyes. This also can be explained by assuming the energy-transfer process where excitation energy is produced through the near-field dipole–dipole interaction (Föster transfer process). The absorption spectra directly reflect the optical transition probability.

The process of photoelectron emission usually occurs when the chemical substrate undergoes internal energy transitions before re-emitting the energy from the absorption event. There is a competition between the charge separation process and deactivation processes occurring in the dye molecules, and the study of a dye's ability for photoconversion is usually accompanied by basic spectroscopic investigations that give information on radiative or non-radiative deactivation of the dye's excited states

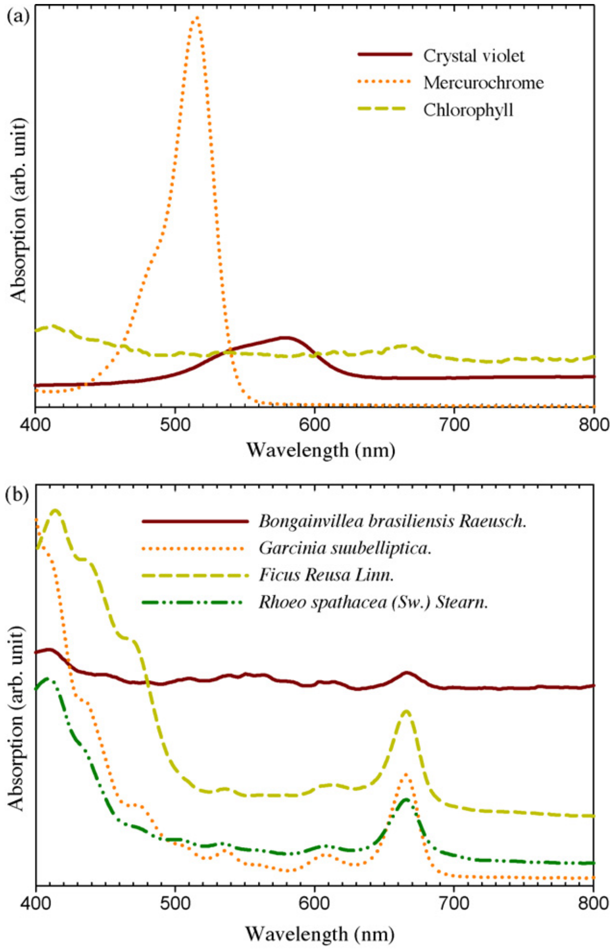

Fig. 5. Absorption spectra of (a) three kinds of commercial dyes and (b) four kinds of natural dyes for the water-based DSSC.

[24]. Thus, both a higher number of π electrons and their delocalization lead to an improvement in the photocurrent generation. The absorption spectrum exhibits a broadband, having a tail in the longer-wavelength region [26].

Synthesis of dyes with broader spectral response has been attempted as a possible strategy. Fig. 5b shows the absorption spectra of *Bongainvillea brasiliensis* Raeusch., *Garcinia suubelliptica.*, *Ficus Reusa* Linn., and *Rhoeo spathacea* (Sw.) Stearn. It can be seen that they have the same absorbent peak, except for *Bongainvillea brasiliensis* Raeusch., with a small variation of absorbance. The other three dyes also have the characteristic peaks of chlorophyll and non-chlorophyll. There are many non-chlorophyll accessory pigments, such as carotenoids or phycobiliproteins, which also absorb light and transfer that light energy to the photosystem chlorophylls. The different chlorophyll and non-chlorophyll pigments associated with the photosystems all have different spectra, either because the spectra of the different chlorophyll pigments are modified by their local protein environment, or because the accessory pigments that have intrinsically different absorption spectra form chlorophyll. The net result is that in vivo the total absorption spectrum is broadened and flattened so that a wider range of red, orange, yellow and blue light can be absorbed by plants. For example, the characteristic absorption peak of chlorophyll has a wavelength of about 430 nm, while the characteristic absorption peak of carotenoid has a wavelength of about 455 nm [4].

The absorption peaks of the commercial chlorophyll dye and the natural dye are centered at the wavelengths of about 665 and 670 nm, respectively. The absorption peak of commercial chlorophyll exhibits red shift (i.e. bathochromic shift) compared with that of the natural dye. Chlorophyll is a well-known compound for photosynthesis, whose molecule has a porphyrin skeleton similar to heme, incorporating Mg^{2+} with a closed shell [26]. The chlorophyll molecules tend to aggregate in polar solvents [27], and both exhibit bathochromic shift upon aggregation.

3.3. Photoelectron emission of various kinds of the commercial and natural dyes in the water-based DSSC

Photoluminescence is a process in which a chemical compound absorbs a photon (electromagnetic radiation), thus transitioning to a higher electronic energy state, and then radiates a photon back out, returning to a lower energy state. Ultimately, available chemical energy states and allowed transitions between states (and therefore wavelengths of light preferentially absorbed and emitted) are determined by the rules of quantum mechanics [28]. In this respect, there may be a correlation between the phenomenon of photoelectron emission and the photoelectric property in a water-based DSSC system.

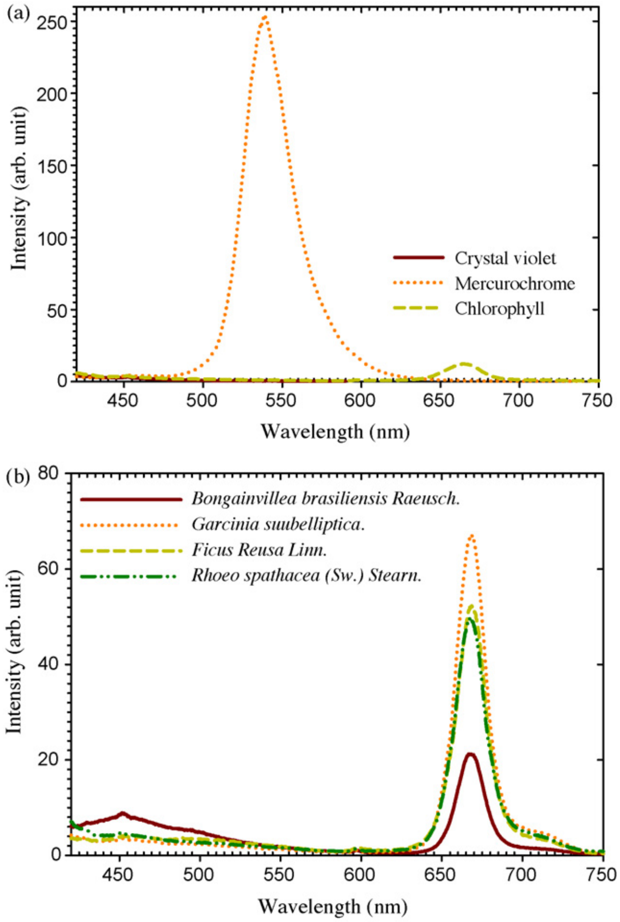

Fig. 6. Emission intensity of (a) three kinds of commercial dyes and (b) four kinds of natural dyes for the water-based DSSC.

Fig. 6 shows the emission intensity of three kinds of commercial dyes (Fig. 6a, crystal violet, mercurochrome, and chlorophyll) and four kinds of natural dyes (Fig. 6b, *Bongainvillea brasiliensis* Raeusch., *Garcinia suubelliptica.*, *Ficus Reusa* Linn., and *Rhoeo spathacea* (Sw.) Stearn.), with kelp extracts in alcohol. Looking at the emission intensity of the commercial dyes in Fig. 6a, mercurochrome has an intensity of 540 nm while crystal violet shows no emission, and exhibits little or no photoluminescence. Although chlorophyll has bright fluorescence at 673 nm [29], this is not obviously observed when compared with the emission intensity of the natural dye in Fig. 6b.

Fig. 6b shows the emission intensity of *Bongainvillea brasiliensis* Raeusch., *Garcinia suubelliptica.*, *Ficus Reusa* Linn., and *Rhoeo spathacea* (Sw.) Stearn. There is the same trend of emission intensity centered at 450 and 670 nm. The emission intensity of chlorophyll exhibits a little red shift and the smaller photoluminescence compared with that of the natural dyes. The chlorophyll molecules may tend to aggregate in polar solvents, and upon aggregation, both absorption and PL spectra exhibit bathochromic shift [24,30].

3.4. Photoelectric property in water-based DSSC sensitized by various kinds of commercial and natural dyes

In DSSC, the current–voltage curve of a solar cell yields important operational parameters [31], among which are the short-circuit current I_{sc}, the open-circuit voltage V_{oc}, the current I_{mp}, and voltage V_{mp}, at the maximum power point, P_{max}.

The fill factor (ff) is calculated as

$$\mathrm{ff} = \frac{P_{\max}}{V_{\mathrm{oc}} I_{\mathrm{sc}}} = \frac{V_{\mathrm{mp}} I_{\mathrm{mp}}}{V_{\mathrm{oc}} I_{\mathrm{sc}}} \tag{2}$$

The solar conversion efficiency (η) is given by

$$\eta = \frac{P_{\max}}{P_{\mathrm{s}}} = \frac{\mathrm{ff} \times V_{\mathrm{oc}} \times J_{\mathrm{sc}}}{P_{\mathrm{s}}} \tag{3}$$

where P_{s} is the input solar irradiance (e.g., 100 mW/cm^2).

The current–voltage curves obtained with the water-based DSSC sensitized by the three kinds of commercial dyes (crystal violet, mercurochrome, and chlorophyll) and four kinds of natural dyes (*Bongainvillea brasiliensis* Raeusch., *Garcinia suubelliptica.*, *Ficus Reusa* Linn., and *Rhoeo spathacea* (Sw.) Stearn.) are shown in Fig. 7.

In Fig. 7a, the *I–V* curve obtained with the water-based DSSC sensitized by crystal violet is inferior to those obtained by mercurochrome or chlorophyll due to the absorbance or photoluminescence property. The photoelectric properties of *Bongainvillea brasiliensis* Raeusch., *Garcinia suubelliptica.*, *Ficus Reusa* Linn., and *Rhoeo spathacea* (Sw.) Stearn. seen in Fig. 7b have the same trend of *I–V* curves, which are superior to those obtained by the three commercial dyes in this study. The results show that the natural dyes, adsorbed onto the TiO_2 photoelectrode, absorb visible light and promote electron transfer across the dye/semiconductor interface. Conversion of visible light into electricity by sensitization of TiO_2 with readily obtained natural dyes is an encouraging alternative which needs to be further developed [1]. Since the carbonyl and hydroxyl groups presented on anthocyanin molecules, they can be bound to the surface of the TiO_2 film, which is capable of chelating to the Ti(IV) sites of the TiO_2 surface and thus favors the photoelectric conversion effect [32]. The other reason for the decrease in the photocurrent sensitized by the commercial dyes is due to the high thermal relation of these dyes when they are aggregated or mixed together [24]. Creation of aggregated dye species leads to a decrease in the photoconversion process, since in aggregated dyes absorbed energy is mostly changed into heat, and thus lost in the thermal process rather than used for charge separation.

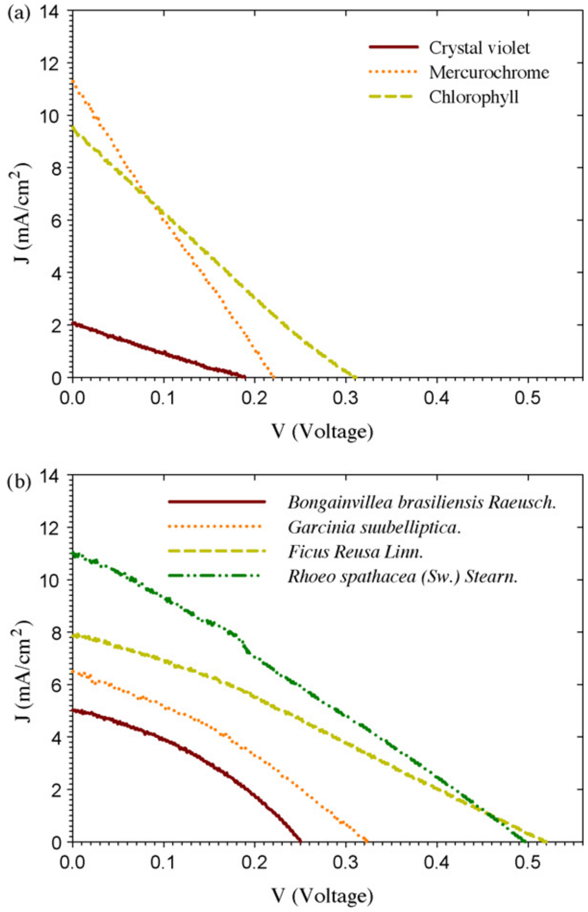

Fig. 7. *I–V* curves obtained with the water-based DSSC sensitized by the (a) three kinds of commercial dyes and (b) four kinds of natural dyes.

Table 1 presents the photoelectrochemical data obtained with the water-based DSSC sensitized by various kinds of commercial and natural dyes. Crystal violet, mercurochrome, and chlorophyll were employed as commercial sensitizers in water-based DSSC, resulting in I_{sc} and V_{oc} values ranging from 0.188 to 0.308 V and 2.04 to 11.3 mA/cm^2, respectively. *Bongainvillea brasiliensis* Raeusch., *Garcinia suubelliptica.*, *Ficus Reusa* Linn., and *Rhoeo spathacea* (Sw.) Stearn. were employed as natural sensitizers in water-based DSSC, resulting in I_{sc} and V_{oc} values ranging from 0.249 to 0.520 V and 5 to 10.9 mA/cm^2, respectively. It is evident that the short-circuit current or the open-circuit voltage of water-based DSSC sensitized by the commercial dyes are lower than those sensitized by the natural dyes. Therefore, the efficiencies of photoelectric conversion of water-based DSSC sensitized by the natural dyes are higher than those sensitized by the commercial dyes. The fill factor values ranging from 24.07 to 25.91 and 27.39 to 36.44 were obtained with the commercial dyes and the natural dyes, respectively. The maximum power point values

Table 1
Photoelectrochemical data obtained with the water-based DSSC sensitized by various kinds of commercial and natural dyes

Dye	V_{oc} (V)	I_{sc} (mA/cm^2)	ff (%)	$P_{\max}$ (μW)	η (%)
Crystal violet	0.188	2.04	25.91	99.7	0.0997
Mercurochrome	0.221	11.3	24.79	617	0.617
Chlorophyll	0.308	9.51	24.07	705	0.705
Bongainvillea brasiliensis Raeusch.	0.249	5	36.44	454	0.454
Garcinia suubelliptica.	0.322	6.48	33.14	691	0.691
Ficus Reusa Linn.	0.520	7.85	28.92	1180	1.18
Rhoeo spathacea (Sw.) Stearn.	0.496	10.9	27.39	1490	1.49

obtained for these natural dyes (454–1490 μW) are superior to those obtained for the commercial dyes (99.7–705 μW), except for chlorophyll. Porphyrins constitute a class of molecules that contain four pyrrole rings linked by the methane carbon bridge, which enhance the characteristics of photovoltaics for the natural pigments in water-based DSSC. Various kinds of dyes from *Bongainvillea brasiliensis* Raeusch., *Garcinia suubelliptica.*, *Ficus Reusa* Linn., and *Rhoeo spathacea* (Sw.) Stearn. are natural pigments, with a molecular structure based on the porphyrin skeleton of chlorophyll [24], and they have been shown to be promising dyes for photovoltaics [33,34]. The solar conversion efficiency of the water-based DSSC sensitized by *Rhoeo spathacea* (Sw.) Stearn. can reach 1.49% with $I_{sc} = 10.9$ mA/cm^2 and $V_{oc} = 0.496$ V under irradiation of 100 mW/cm^2, which is the highest photosignal in this study. These four natural sensitizers applied in water-based DSSC are thus suitable for use to improve the efficiency of environmentally friendly energy devices.

4. Conclusions

An Au NP's layer in water-based DSSC with the aqueous electrolyte of Ce$^{4+/3+}$ system can act as a Schottky barrier to improve the efficiency of photoelectric conversion. Low-cost and environmental-friendly natural dyes present good light harvesting and good photoelectric properties on a TiO_2 photoelectrode loaded with Au NPs. The use of a natural source enables a faster, simpler and more environmentally friendly production of solar cells, and provides an interesting alternative to commercial synthetic dyes. This strategy is suitable for application in the field of water-based DSSC.

Acknowledgments

The work was financially supported by the National Science Council of Taiwan, the Republic of China, grants no.: NSC 96-2221-E-006-007 and NSC 96-2221-E-020-013, which are gratefully acknowledged. The authors would like to thank Ms. L.C. Wang in National Sun Yat-sen University for HRTEM/electron diffraction pattern photographs.

References

[1] C.G. Garcia, A.S. Polo, N.Y.M. Iha, J. Photochem. Photobiol. A 160 (2003) 87.
[2] K. Kalyanasundaram, M. Grätzel (Eds.), Photosensitization and Photocatalysis Using Inorganic and Organometallic Compounds, Kluwer Academic Publishers, Dordrecht, 1993.
[3] J.A. Bard, M.A. Fox, Acc. Chem. Res. 28 (1995) 141.
[4] S. Hao, J. Wu, Y. Huang, J. Lin, Sol. Energy 80 (2006) 209.
[5] B. O'Regan, J. Moser, M. Anderson, M. Grätzel, J. Phys. Chem. 94 (1990) 8720.
[6] T.N. Murakami, H. Saito, S. Uegusa, N. Kawashima, T. Miyasaka, Chem. Lett. 32 (2003) 1154.
[7] S. Link, M.A. El-Sayed, J. Phys. Chem. B 103 (1999) 8410.
[8] R. Jin, Y.C. Cao, C.A. Mirkin, K.L. Kelly, G.C. Schatz, J.G. Zheng, Science 294 (2001) 1901.
[9] E.A. Stern, R.A. Ferrell, Phys. Rev. 111 (1958) 1214.
[10] R.H. Ritchie, H.B. Eldridge, Phys. Rev. 126 (1962) 1947.
[11] M.J.Y. Jarvis, V. Blagojevic, G.K. Koyanagi, Chem. Phys. Lett. 416 (2005) 268.
[12] Y.C. Liu, C.C. Yu, C.C. Wang, Chem. Phys. Lett. 420 (2006) 245.
[13] P.V. Kazakevich, A.V. Simakin, G.A. Shafeev, Chem. Phys. Lett. 421 (2006) 348.
[14] E.W. McFarland, J. Tang, Nature 421 (2003) 616.
[15] N. Chandrasekharan, P.V. Kamat, J. Phys. Chem. B 104 (2000) 10851.
[16] Y. Tian, T. Tatsuma, J. Am. Chem. Soc. 127 (2005) 7632.
[17] K. Yu, Y. Tian, T. Tatsuma, Phys. Chem. Chem. Phys. 8 (2006) 5417.
[18] Y. Tian, H. Notsu, T. Tatsuma, Photochem. Photobiol. Sci. 4 (2005) 598.
[19] Y. Tian, T. Tatsuma, Chem. Commun. (2004) 1810.
[20] Y.H. Su, W.H. Lai, L.G. Teoh, M.H. Hon, J.L. Huang, Appl. Phys. A 88 (2007) 173.
[21] M. Grätzl, Nature 414 (2001) 338.
[22] K. Chiang, R. Amal, T. Tran, Adv. Environ. Res. 6 (2002) 471.
[23] C. Kittel, Introduction to Solid State Physics, John Wiley & Sons, Canada, 1976.
[24] D. Wróbel, CR Chim. 6 (2003) 417.
[25] C. Sahoo, A.K. Gupta, A. Pal, Dyes Pigments 66 (2005) 189.
[26] H. Tajima, K. Shimatani, T. Komino, S. Ikeda, M. Matsuda, Y. Ando, H. Akiyama, Colloid Surf. A: Physicochem. Eng. Aspects 284 (2006) 61.
[27] H. Furukawa, T. Oba, H. Tamiaki, T. Watanabe, J. Phys. Chem. B 103 (1999) 7398.
[28] A. Donald, McQuarrie, D.S. John, Physical Chemistry: A Molecular Approach, University Science Books, 1997.
[29] T.M. Liu, S.W. Chu, C.K. Sun, B.L. Lin, P.C. Cheng, I. Johnson, Scanning 23 (2001) 249.
[30] K. Shimatani, H. Tajima, T. Komino, S. Ikeda, M. Matsuda, Chem. Lett. 34 (2005) 948.
[31] G.P. Smestad, Optoelectronics of Solar Cells, SPIE—The International Society for Optical Engineering, Bellingham, Washington, 2002.
[32] Q. Dai, J. Rabani, Chem. Commun. 2142 (2001).
[33] A. Ptak, E. Chrzumnicka, A. Planner, D. Frackowiak, Biophys. Chem. 65 (1997) 165.
[34] A. Ptak, E. Chrzumnicka, A. Dudkowiak, D. Frackowiak, J. Photochem. Photobiol. A: Chem. 98 (1996) 159.